Chemically Induced Morphogenesis of P22 Virus like Particles by the Surfactant Sodium Dodecyl Sulfate

Ekaterina Selivanovitch1, Ranjit Koliyatt1, Trevor Douglas1*

A.

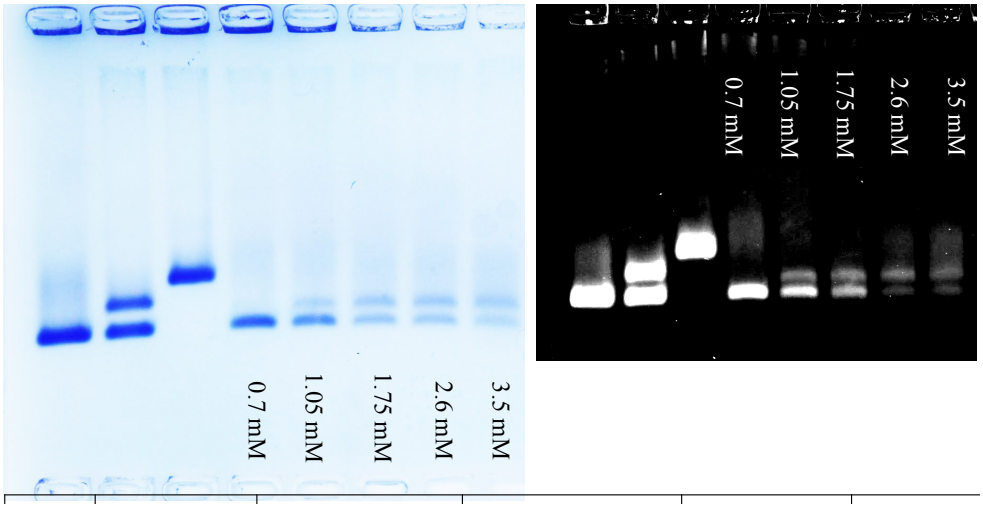

B.

Lane	SDS Conc	Protein Conc	Ratio SDS:CP	EX Count	PC Count
1	PC	0.5mg/mL	None		
2	(EX) Heat	0.5mg/mL	None	2.23E+06	2.35E+06
3	WB	0.5mg/mL	None		
4	0.7 mM	0.5mg/mL	77.00	0	1.50E+06
5	1.05 mM	0.5mg/mL	115.00	2.93E+05	7.12E+05
6	1.75 mM	0.5mg/mL	192.00	4.54E+05	5.21E+05
7	2.6 mM	0.5mg/mL	288.00	3.57E+05	2.56E+05
8	3.5 mM	0.5mg/mL	384.00	3.27E+05	49960

C.

MW of Particle	Contribution of CP	Contribution of SP	MW SP
23.5MDa	19.6MDa	3.9MDa	33.6KDa

D.

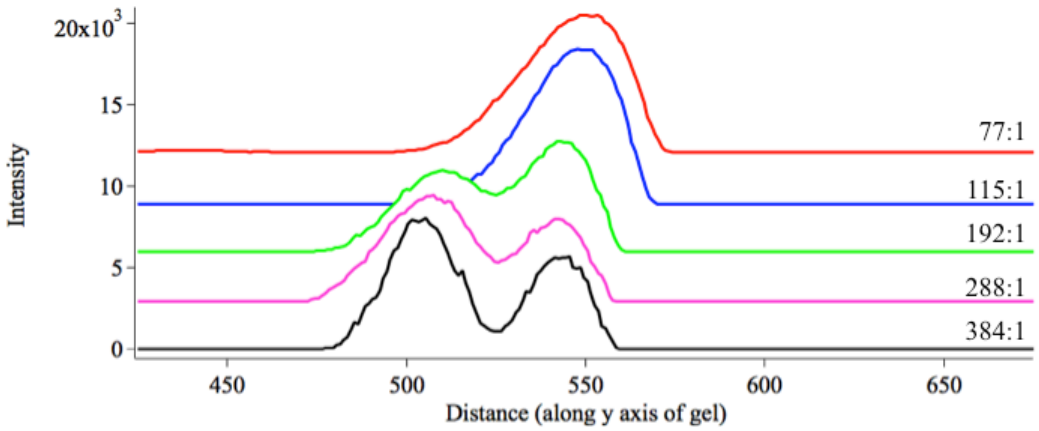

E.

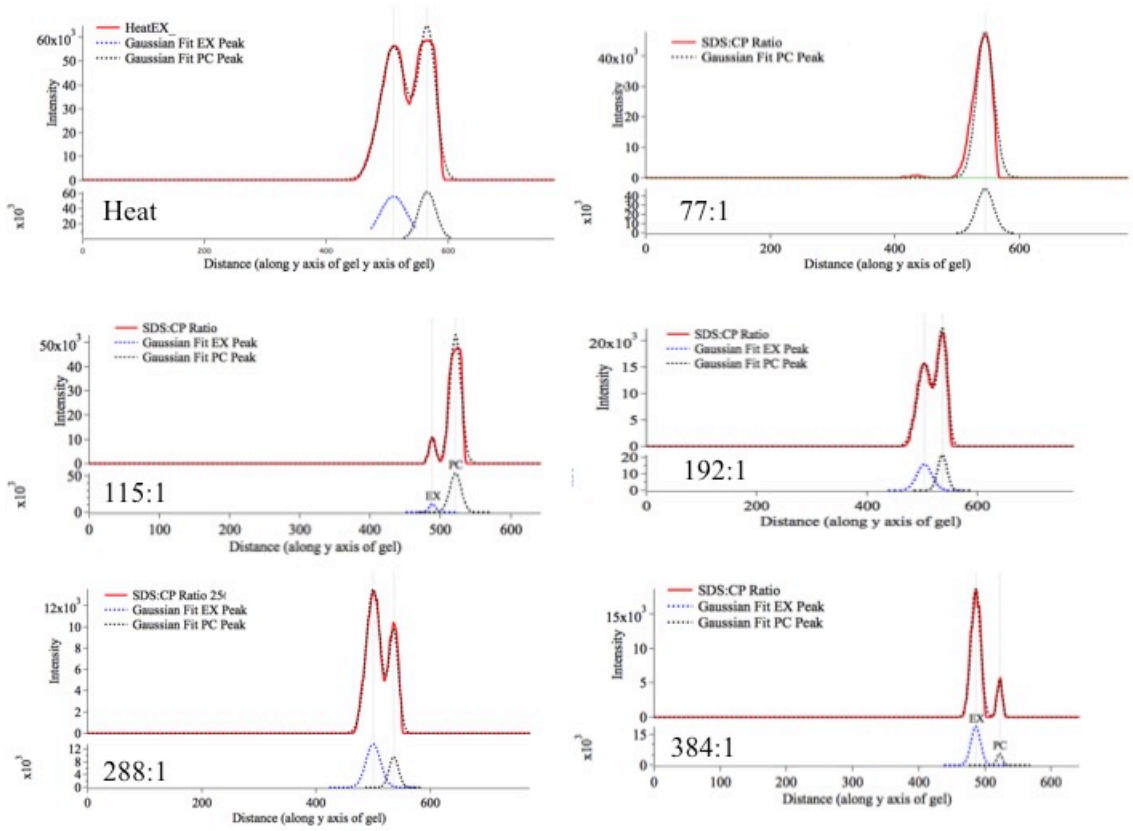

Supplementary Figure 1: Characterization of P22 wtSP (wtCP/wtSP). A) P22 wtSP Native agarose gel and inverted image that was processed using ImageJ2 with SDS concentrations listed at the bottom. B) Table displaying the data that was obtained from densitometry analysis of the gel above. The relative populations of PC and EX were calculated from the peaks displayed in part D using the IgorPro Peak Area macro. C) MW of P22 wtSP was obtained using SEC-MALS and the rest are theoretical values calculated using the amino acid sequence. D) Line profile scan of the gel displayed in A. The peak areas have been normalized to reflect the relative populations of EX and PC particles in the samples. E) Plots acquired by plotting the intensity of each lane, with the ratios displayed on each plot corresponding to their respective lanes found in table B of this figure.

A.

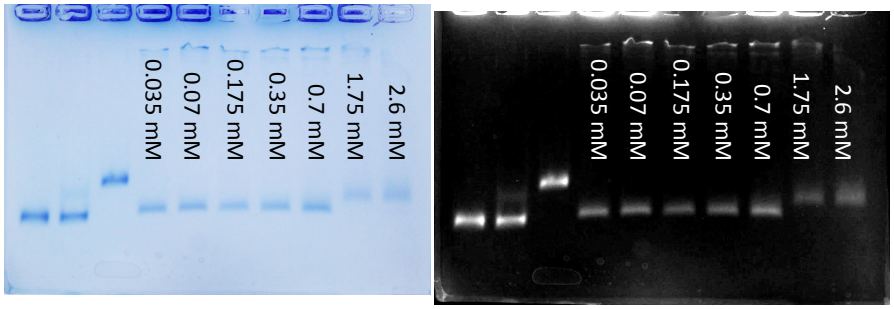

B.

Lane	SDS Conc	Protein Conc	Ratio SDS:CP	EX Count	PC Count
1	PC	0.5mg/mL	None		
2	(EX) Heat	0.5mg/mL	None	5.73E+05	1.62E+06
3	WB	0.5mg/mL	None		
4	0.035 mM	0.5mg/mL	5.00	0%	100%
5	0.07 mM	0.5mg/mL	10.00	0%	100%
6	0.175 mM	0.5mg/mL	25.00	100%	0%
7	0.35 mM	0.5mg/mL	50.00	100%	0%
8	0.7 mM	0.5mg/mL	100.00	100%	0%
9	1.75 mM	0.5mg/mL	250.00	100%	0%
10	2.6 mM	0.5mg/mL	377.00	100%	0%

C.

MW of Particle	Contribution of CP	Contribution of SP	MW SP
30.5MDa	19.6MDa	10.9MDa	50.6KDa

D.

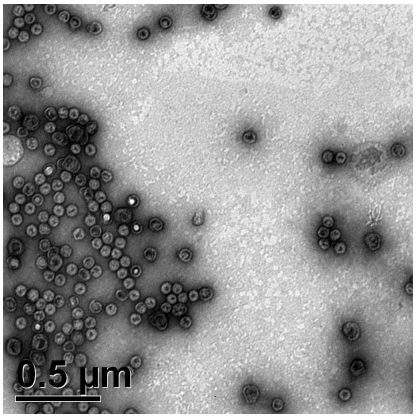

E.

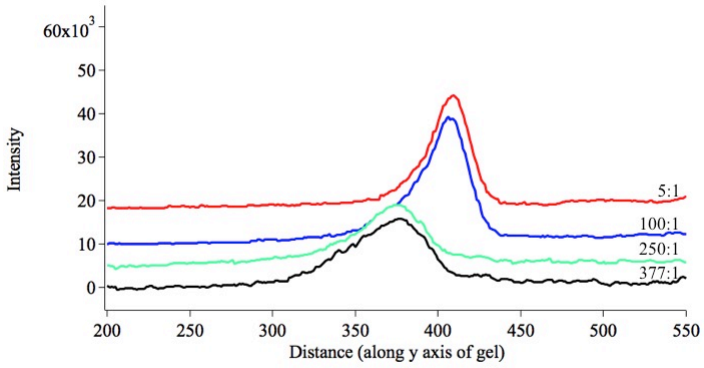

F.

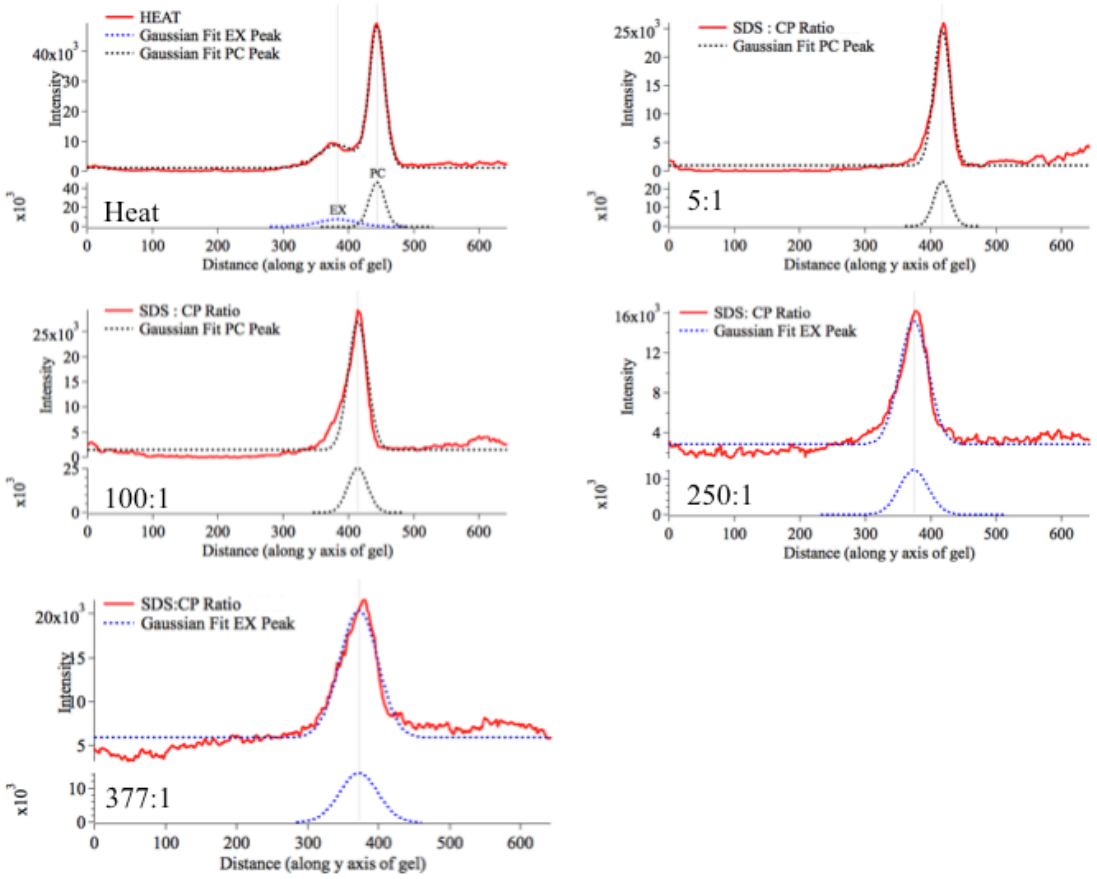

Supplementary Figure 2: Characterization of P22 AdhD-SP (wtCP/AdhD-SP). A) Native gel with samples incubated with SDS concentrations labeled below gel. B) Information on the samples in each lane displayed in A. C) MW data on P22 AdhD-SP. D) TEM image of a P22 AdhD-SP sample expanded using SDS. E) Line profile scan of the gel displayed in A. F) Densitometry analysis of lanes displayed in B. There were no species in the gel that had a mixed population of particles in the EX and PC morphologies, except for the sample in lane 2, which was treated with heat. Therefore the counts are displayed in the form of percentages, rather than a relative count. The densitometry graphs pertaining to lanes 5-7 are not shown because there is no change between the bands in lane 4 versus lane 8. Going from graph of lane 8 (100:1) to graph in lane 9 (250:1), there is a clear shift of the peak from 420 to 380, coinciding with the band shift seen in the gel displayed in A.

A.

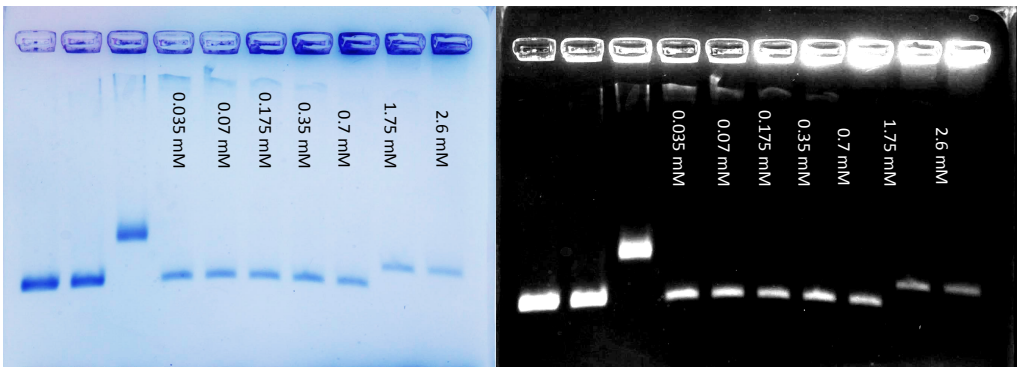

B.

Lane	SDS Conc	Protein Conc	Ratio SDS:CP	EX Count	PC Count
1	PC	0.5mg/mL	None		
2	(EX) Heat	0.5mg/mL	None	7.38E+05	3.20E+06
3	WB	0.5mg/mL	None		
4	0.035 mM	0.5mg/mL	5	0%	100%
5	0.07 mM	0.5mg/mL	10	0%	100%
6	0.175 mM	0.5mg/mL	26	100%	0%
7	0.35 mM	0.5mg/mL	52	100%	0%
8	0.7 mM	0.5mg/mL	104	100%	0%
9	1.75 mM	0.5mg/mL	260	100%	0%
10	2.6 mM	0.5mg/mL	391	100%	0%

C.

MW of Particle	Contribution of CP	Contribution of SP	MW SP
31.6MDa	19.6MDa	12.0MDa	46.3KDa

D.

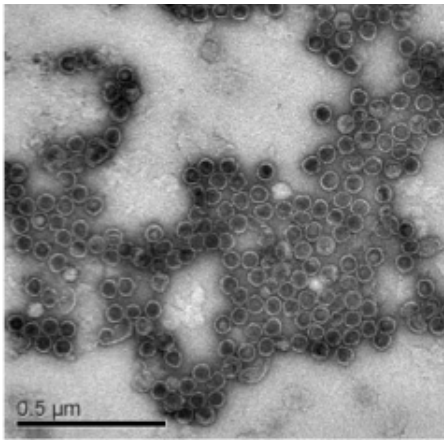

E.

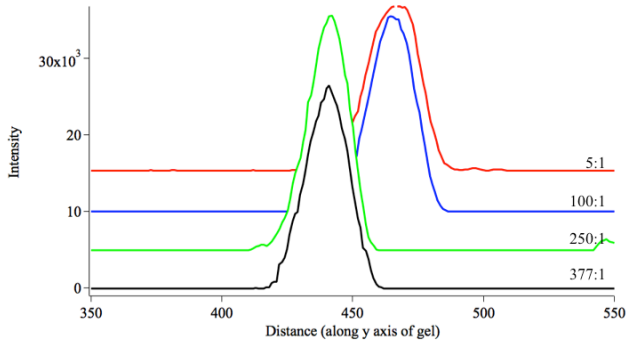

F.

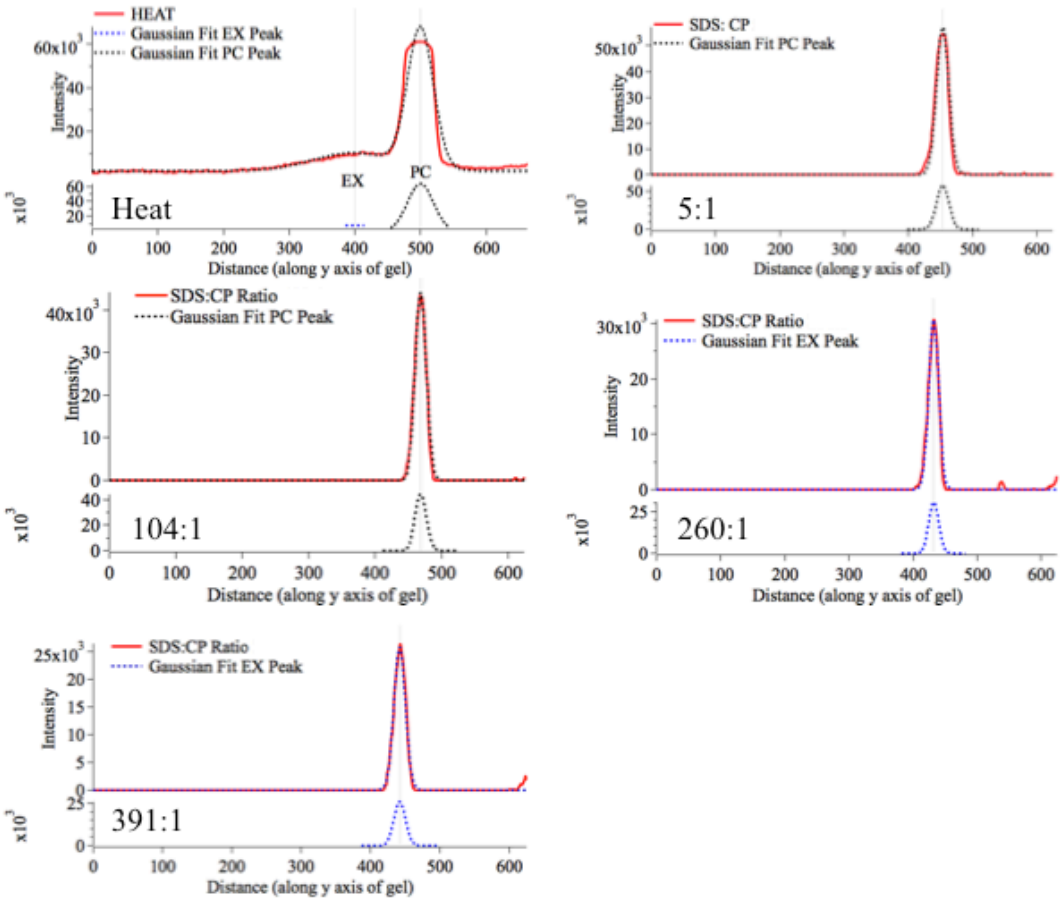

Supplementary Figure 3: Characterization of P22 GFP-SP (wtCP/GFP-SP). A) Native gel with samples incubated with SDS concentrations labeled below gel. B) Information on the samples in each lane displayed in A. C) MW data on P22 GFP-SP. D) TEM image of a P22 GFP-SP sample expanded using SDS. E) Line profile scan of the gel displayed in A. The peak areas have been normalized to see the relative band shift F) Densitometry analysis of lanes displayed in B. There were no species in the gel that had a mixed population of particles in the EX and PC morphologies, except for the sample in lane 2, which was treated with heat. Therefore the counts are displayed in the form of percentages, rather than a relative count. The densitometry graphs pertaining to lanes 5-7 are not shown. Going from graph of lane 8 (104:1) to graph in lane 9 (260:1), there is a clear shift of the peak from 460 to 440, coinciding with the band shift seen in the gel displayed in A.

A.

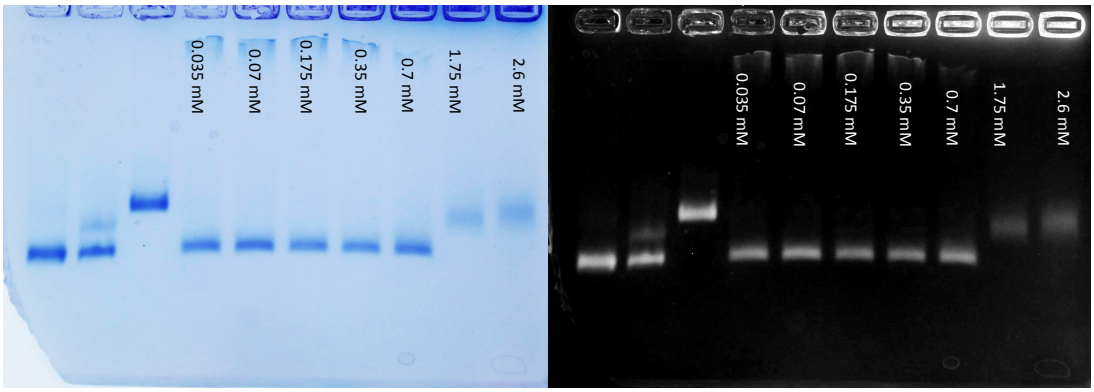

B.

Lane	SDS Conc	Protein Conc	Ratio SDS:CP	EX Count	PC Count
1	PC	0.5mg/mL	None		
2	(EX) Heat	0.5mg/mL	None	3.70E+05	1.10E+06
3	WB	0.5mg/mL	None		
4	0.035 mM	0.5mg/mL	5	0%	100%
5	0.07 mM	0.5mg/mL	10	0%	100%
6	0.175 mM	0.5mg/mL	24	100%	0%
7	0.35 mM	0.5mg/mL	48	100%	0%
8	0.7 mM	0.5mg/mL	96	100%	0%
9	1.75 mM	0.5mg/mL	240	100%	0%
10	2.6 mM	0.5mg/mL	360	100%	0%

C.

MW of Particle	Contribution of CP	Contribution of SP	MW SP
29.1MDa	19.6MDa	9.5MDa	19.9KDa

D.

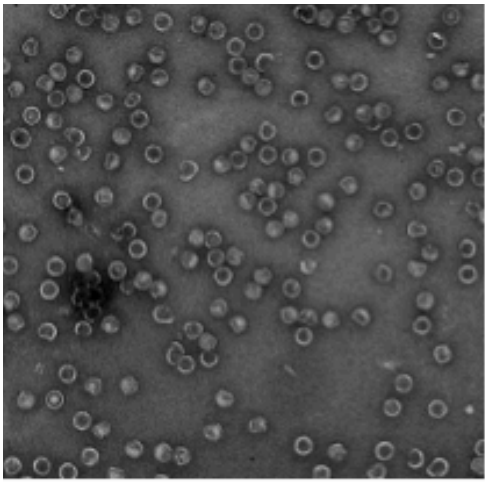

E.

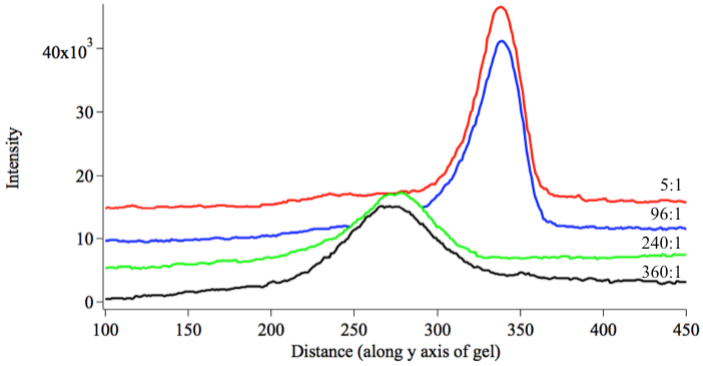

F.

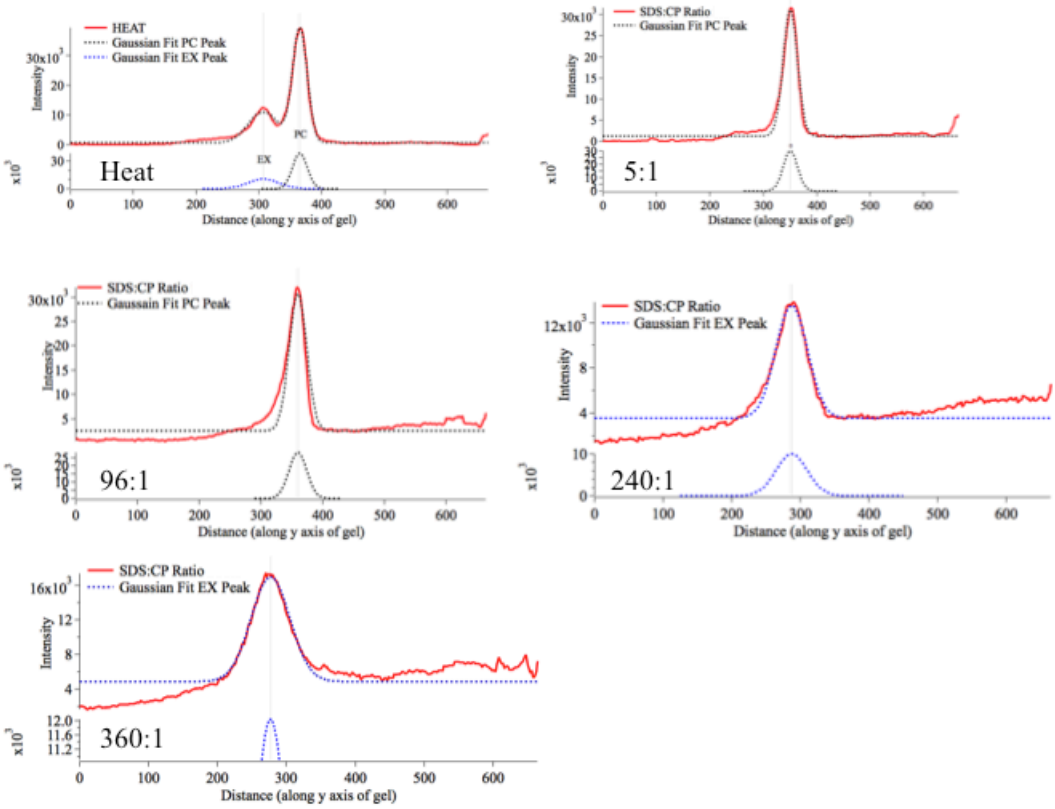

Supplementary Figure 4: Characterization of P22 SP-141 (wtCP/SP142-303). A) Native gel with samples incubated with SDS concentrations labeled below gel. B) Information on the samples in each lane displayed in A. C) MW data on P22 SP141. D) TEM image of a P22 SP-141 sample expanded using SDS. E) Line profile scan of the gel displayed in A. F) Densitometry analysis of lanes displayed in B. There were no species in the gel that had a mixed population of particles in the EX and PC morphologies, except for the sample in lane 2, which was treated with heat. Therefore the counts are displayed in the form of percentages, rather than a relative count. The densitometry graphs pertaining to lanes 5-7 are not shown. Going from graph of lane 8 (96:1) to graph in lane 9 (240:1), there is a clear shift of the peak from 350 to 290, coinciding with the band shift seen in the gel displayed in A.

A.

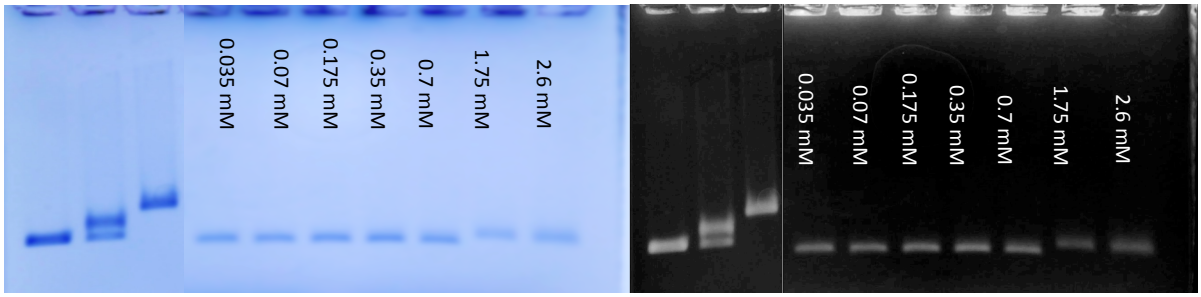

B.

Lane	SDS Conc	Protein Conc	Ratio SDS:CP	EX Count	PC Count
1	PC	0.5mg/mL	None		
2	(EX) Heat	0.5mg/mL	None	5.69E+03	2.57E+03
3	WB	0.5mg/mL	None		
4	0.035 mM	0.5mg/mL	5	0%	100%
5	0.07 mM	0.5mg/mL	10	0%	100%
6	0.175 mM	0.5mg/mL	26	100%	0%
7	0.35 mM	0.5mg/mL	52	100%	0%
8	0.7 mM	0.5mg/mL	105	100%	0%
9	1.75 mM	0.5mg/mL	260	100%	0%
10	2.6 mM	0.5mg/mL	392	100%	0%

C.

MW of Particle	Contribution of CP	Contribution of SP	MW SP
31.7MDa	19.6MDa	12.1MDa	73.6KDa

D.

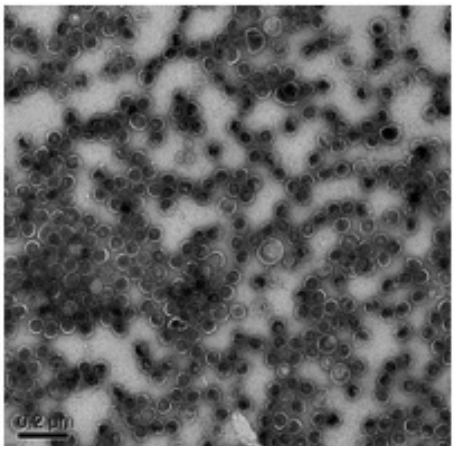

E.

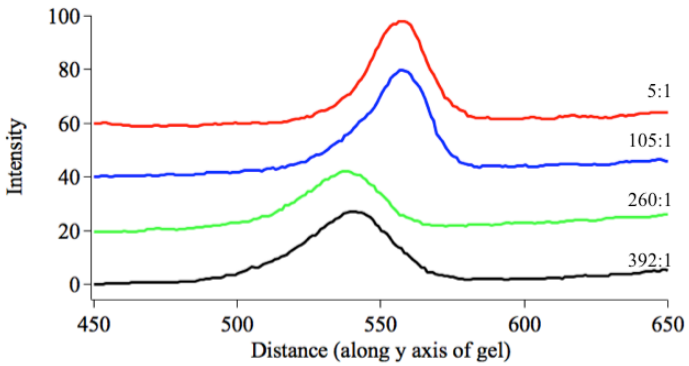

F.

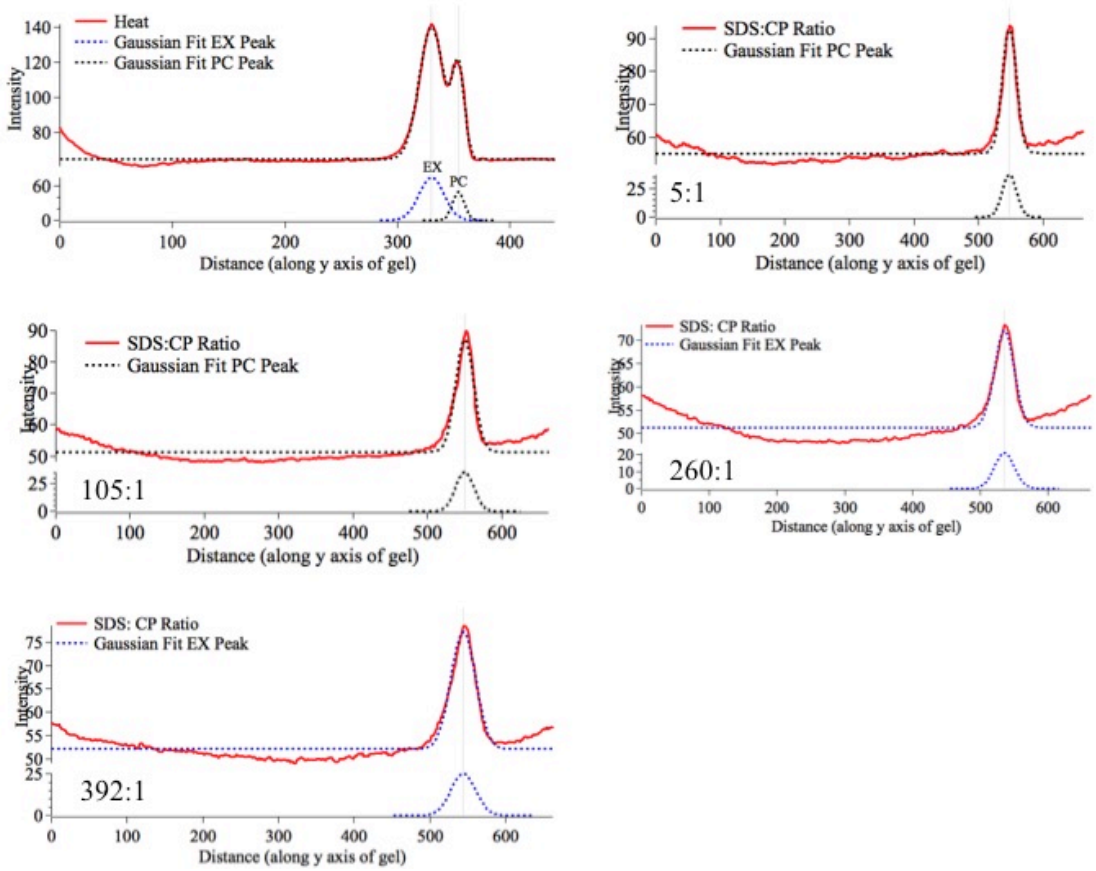

Supplementary Figure 5: Characterization of P22 CelB-SP (wtCP/CelB). A) Native gel with samples incubated with SDS concentrations labeled below gel. B) Information on the samples in each lane displayed in A. C) MW data on P22 CelB-SP. D) TEM image of a P22 CelB-SP sample expanded using SDS. E) Line profile scan of the gel displayed in A. F) Densitometry analysis of lanes displayed in B. There were no species in the gel that had a mixed population of particles in the EX and PC morphologies, except for the sample in lane 2, which was treated with heat. Therefore the counts are displayed in the form of percentages, rather than a relative count. The densitometry graphs pertaining to lanes 5-7 are not shown. Going from graph of lane 8 (105:1) to graph in lane 9 (260:1), there is a clear shift of the peak from 550 to 535, coinciding with the band shift seen in the gel displayed in A.

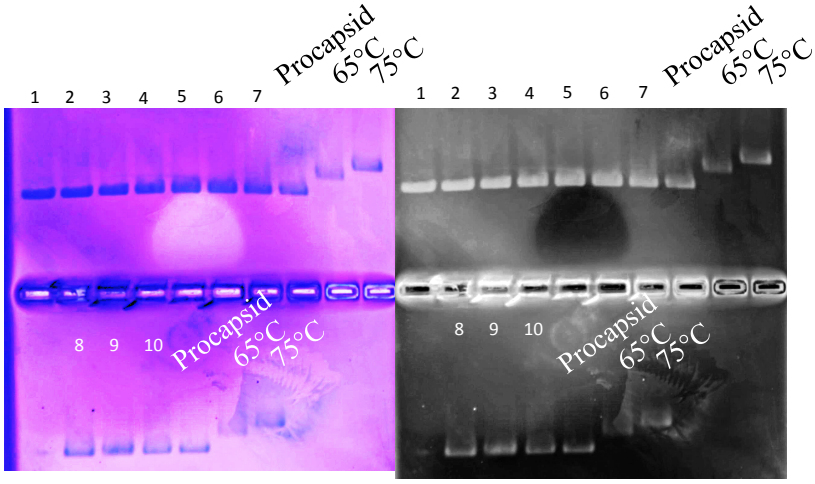

1. 15 min. incubation/ .875 mM SDS
2. 15 min. incubation/ 1.75 mM SDS
3. 15 min. incubation/ 3.5 mM SDS
4. 55 min. incubation/ 3.5 mM SDS
5. 55 min. incubation/ .875 mM SDS
6. 55 min. incubation/ 1.75 mM SDS
7. 100 min. incubation/ 3.5 mM SDS
8. 100 min. incubation/ .875 mM SDS
9. 100 min. incubation/ 1.75 mM SDS
10. 100 min. incubation/ 3.5 mM SDS

Supporting Figure 6: Native agarose gel with P22 ES (Empty Shell: No cargo) variant incubated with SDS for varying times and SDS concentrations. Lane 7 and lane 10 contain P22 incubated for 100 minutes with 0.1% (w/v) concentration of SDS, showing no expansion with the same conditions for which all other variants expanded.

Construct	PI: SP	PI: Sp-Cargo	PI: Cargo	CP
P22 wtSP	5.15			4.97
P22 SP-141	9.4			4.97
P22 GFP-SP	9.4	8.75	6.61	4.97
P22 AdhD-SP	9.4	6.71	5.49	4.97
P22 CelB-SP	9.4	5.94	5.48	4.97

Supporting Figure 7 (Table): The PI values of SP, CP, and any cargo are displayed. In this case cargo refers to either AdhD, GFP, or CelB. The PI values were calculated using Expasy and show that at pH 7 all cargoes are negatively charged.

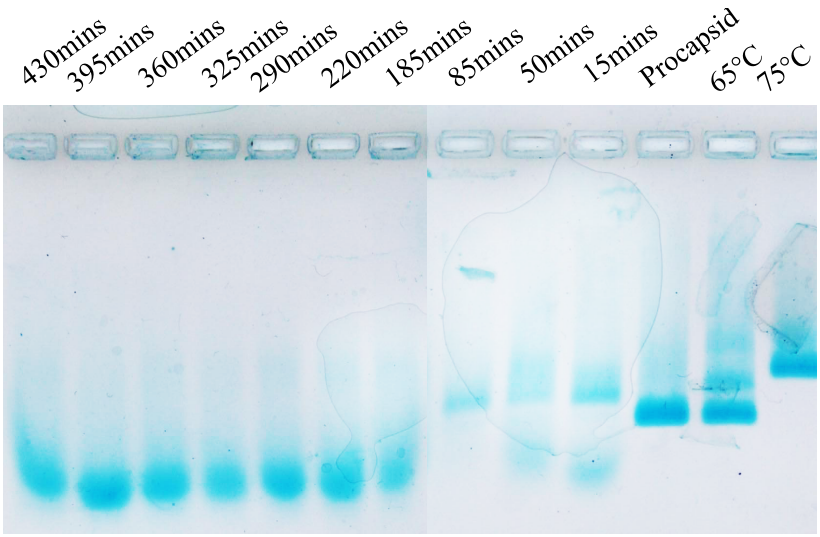

Supporting Figure 8: Native agarose gel with P22 AdhD-SP with increasing incubation times. This determines that with increasing incubation time with 0.1% SDS the particles disassemble.

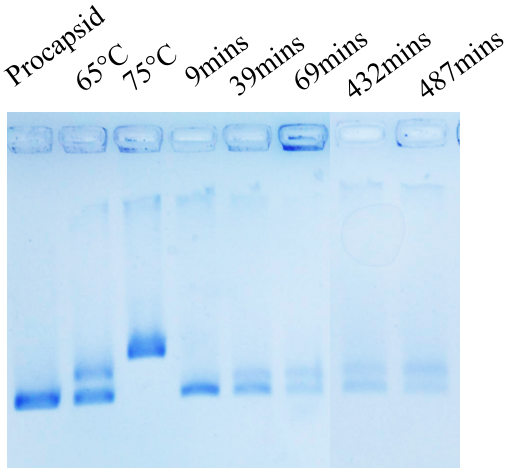

Supporting Figure 9: Native agarose gel with P22 wtSP incubated with 0.05% SDS for increasing incubation time to indicate that it is not a sufficient concentration to expand the entire population of particles in solution.

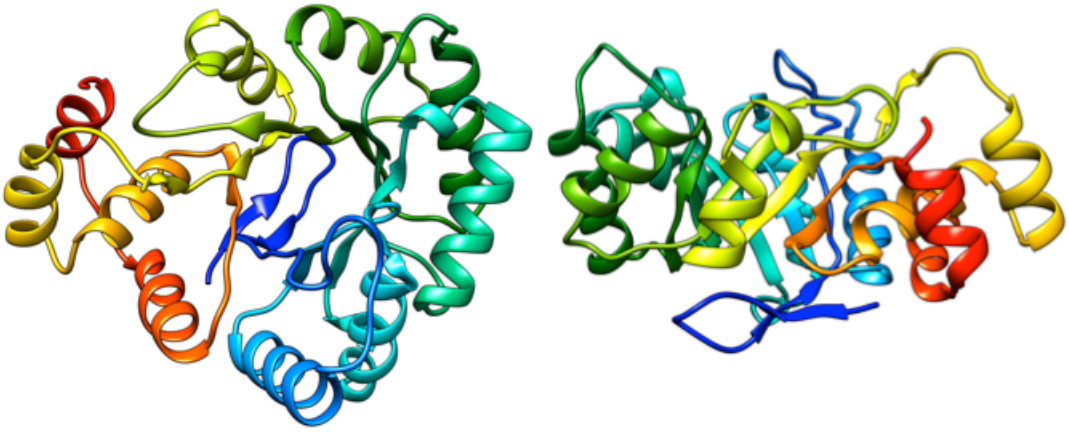

Supporting Figure 10: Homology model of AdhD. Image is colored by rainbow Blue→Red N terminus→ C terminus. The dimensions of the model are 5.7 nm x 4.8 nm x 4.3 nm. Structure was based on **PDB Molecule:**2,5-diketo-d-gluconic acid reductase. The Phyre2 web portal was used to construct this homology model.[1]

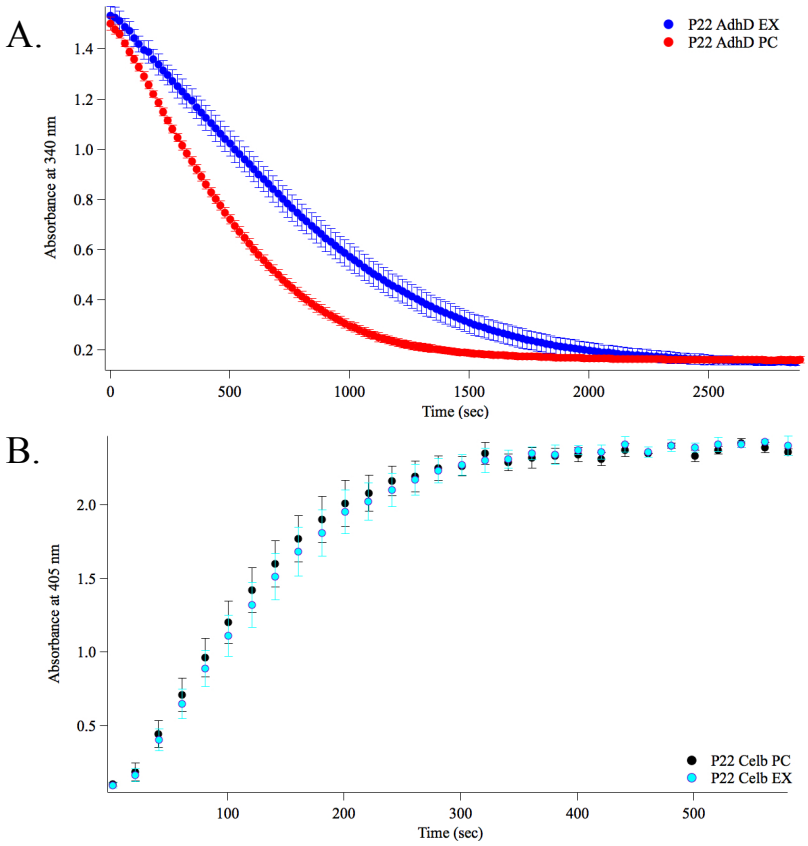

Supporting Figure 11: The P22 variants encapsulating enzyme-cargo were tested for catalytic activity. A) P22 AdhD-SP EX (blue) and PC (red) activities were tested by monitoring absorbance at 340 nm, a characteristic signature of the cofactor NADH. As the NADH is reduced to NAD^+, the peak intensity decreases. A decrease at 340 nm indicates that both the PC and EX P22 particles have enzymatically active AdhD cargo. B) P22 CelB_SP EX (light blue) and PC (black) activities were tested by monitoring absorbance at 405 nm, a characteristic signature of the 4-nitrophenol. As 4-nitrophenyl-β-glucopyronoside (PNPG) releases 4-nitrophenol, the peak intensity increases. A increase at 405 nm indicates that both the PC and EX P22 particles have enzymatically active CelB cargo.

Interface	Symmetry	Buried Surface Area(Å2)	Total # Interfaces	Total Surface Area of interface on P22 Capsid (Å2)
B1-C1	Q-6	6930.5	60	415830
A1-B1	Q-6	6861.4	60	411684
E1-F1	Q-6	6966.5	60	417990
G1-G2	I-5	6911.9	60	414714
A1-F1	Q-6	6690.8	60	401448
D1-E1	Q-6	6744.3	60	404658
C1-D1	Q-6	6792.5	60	407550
E1-F10	Q-3	3292.4	60	197544
D1-D7	I-3	3270.7	60	196242
C2-F1	Q-3	3181.1	60	190866
A1-B2	Q-3	3154.7	60	189282
C1-E7	Q-3	3081.1	60	184866
A1-G2	Q-3	3128.5	60	187710
B1-G1	Q-3	3072	60	184320
D1-E7	Q-2	1578.1	60	94686
B1-G2	Q-2	1461.5	60	87690
A1-C2	Q-2	1389.8	60	83388
F1-F10	I-2	1305.8	30	39174
E1-E10	I-2	716.9	30	21507
B2-F1	Q-2	585.8	60	35148
A1-G1	Q-2	539.5	60	32370
C1-D7	Q-2	555.5	60	33330
C2-E1	Q-6	473	60	28380
F1-G2	Q-6	490.5	60	29430
C7-	Q-6	477.1	60	28626

D1				
B1-E7	Q-6	479.5	60	28770
D1-F10	Q-6	470.1	60	28206
A1-A2	I-5	456.1	60	27366
B2-G1	Q-6	454.2	60	27252
			Total Interfacial Area of Capsid:	**4830027**
			Average Interfacial Area/CP Subunit	**11500**

Supporting Figure 12 (Table): The interfacial areas between the P22 CP subunits adopted from VIPER database. The designations of the interfaces found in column 1 above can be found at http://viperdb.scripps.edu/energy_table.php?VDB=5uu5&layer=. In order to calculate the average interfacial area (or area between CP subunits), we first identified the quantity of each interface per VLP, which can be found in column 4. We then multiplied this value by the area of each interface found in column 3. Summing up all these values provided us with the total interfacial area found in the P22. Although we realize that not every CP-CP interactions exhibit the same interfacial area, in order to get an average per CP, we divided by 420 (total CP subunits) to get the value of 11,500 $Å^2$.

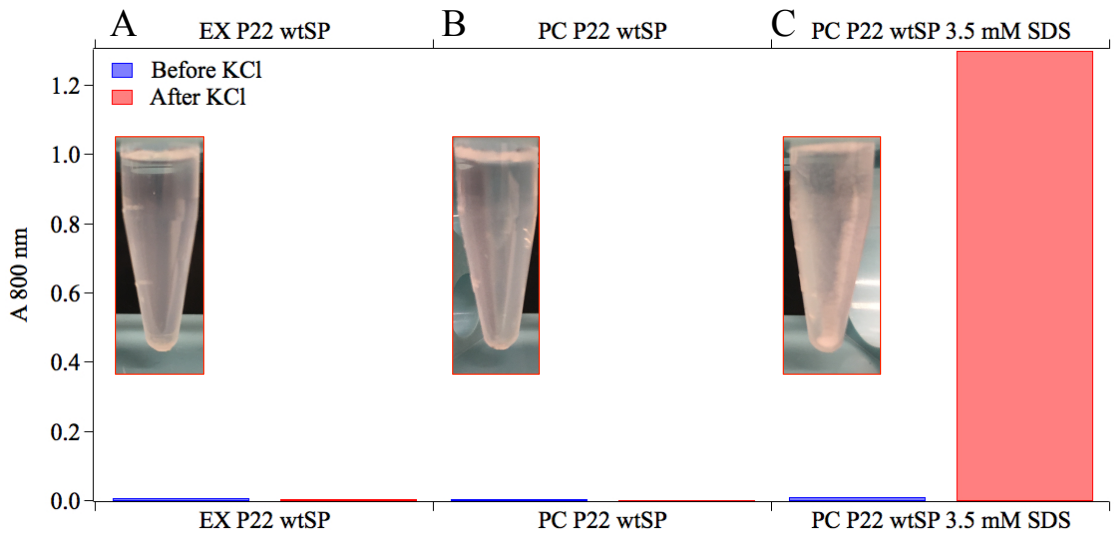

Supporting Figure 13: Potassium Precipitation Assay monitored by scattering at 800 nm using UV-Vis. Absorbance was measured before and after the addition of KCl for each sample. A) Solution containing 0.5 mg/mL of EX P22 VLPs (treated with 3.5 mM SDS, and removed via ultra-centrifugation through a sucrose cushion) and 0.4 M KCl; B) Solution containing 0.5 mg/mL of PC P22 VLPs and 0.4 M KCl ; C) Solution containing 3.5 mM SDS in buffer and 0.4 M SDS. Solutions A and B did not form any precipitates upon addition of KCl, solution C however immediately became turbid from the formation of potassium salts as indicated by monitoring absorbance at 800 nm and the image associated with C. The lack of precipitate in tube B indicates that most of the free SDS molecules have been removed after SDS expansion, and ultra centrifugation is a sufficient method for SDS removal.[2]

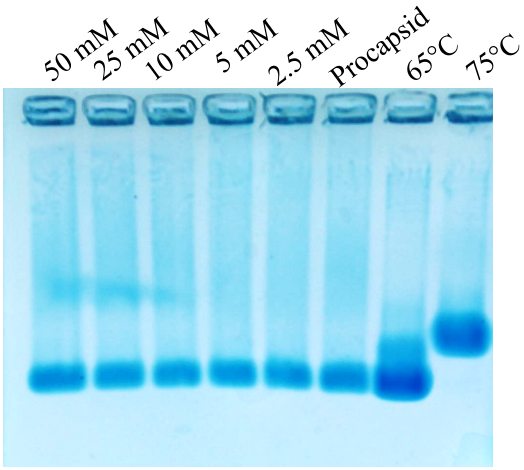

Supporting Figure 14: Treatment of P22 AdhD-SP with Dodecanoic Acid. In order to determine if the expansion trigger was specific to SDS, we exposed P22 VLPs to a surfactant containing a negatively charged head-group and a 12-carbon alkyl chain. After treatment with various concentrations, there were no changes to the migration of the PC band suggesting that this mechanism is specific not only to the charge and length of carbon region, but also to size and shape of the SDS molecule.

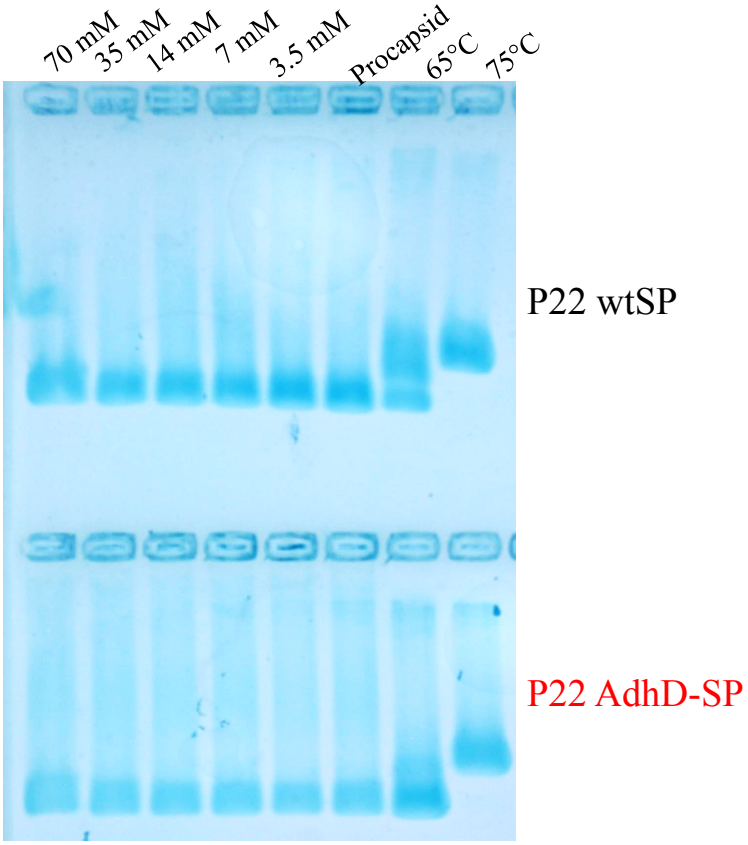

Supporting Figure 15: Treatment of P22 AdhD-SP and P22 wtSP with Sodium Sulfate. In order to determine if electrostatic effects of the sulfate group can result in the same morphogenesis as SDS, we exposed P22 VLPs to sodium sulfate (no alkyl region). After treatment with various concentrations, there were no changes to the migration of the PC band suggesting that this mechanism cannot be triggered via electrostatics alone, and interaction with the alkyl region is critical.

Sequences

Coat Protein (wt)
MALNEGQIVTLAVDEIIETISAITPMAQKAKKYTPPAASMQRSSNTIWMPVEQESP
TQEGWDLTDKATGLLELNVAVNMGEPDNDFFQLRADDLRDETAYRRRIQSAAR
KLANNVELKVANMAAEMGSLVITSPDAIGTNTADAWNFVADAEEIMFSRELNR
DMGTSYFFNPQDYKKAGYDLTKRDIFGRIPEEAYRDGTIQRQVAGFDDVLRSPK
LPVLTKSTATGITVSGAQSFKPVAWQLDNDGNKVNVDNRFATVTLSATTGMKR
GDKISFAGVKFLGQMAKNVLAQDATFSVVRVVDGTHVEITPKPVALDDVSLSPE
QRAYANVNTSLADAMAVNILNVKDARTNVFWADDAIRIVSQPIPANHELFAGM
KTTSFSIPDVGLNGIFATQGDISTLSGLCRIALWYGVNATRPEAIGVGLPGQTA

Scaffolding Protein (wt)
MEPTTEIQATEDLTLSGDHAAASADSLVVDNANDNAGQEEGFEIVLKDDETAPK
QDPAKNAEFARRRIERKRQRELEQQMEAVKRGELPESLRVNPDLPPQPDINAYLS
EEGLAKYDYDNSRALAAFNAANTEWLMKAQDARSNAVAEQGRKTQEFTQQSA
QYVEAARKHYDAAEKLNIPDYQEKEDAFMQLVPPAVGADIMRLFPEKSAALMY
HLGANPEKARQLLAMDGQSALIELTRLSERLTLKPRGKQISSAPPADQPITGDVS
AANKDAIRKQMDAAASKGDVETYRKLKAKLKGIR

AdhD-SP
MAKRVNAFNDLKRIGDDKVTAIGMGTWGIGGRETPDYSRDKESIEAIRYGLELG
MNLIDTAEFYGAGHAEEIVGEAIKEFEREDIFIVSKVWPTHFGYEEAKKAARASA
KRLGTYIDLYLLHWPVDDFKKIEETLHALEDLVDEGVIRYIGVSNFNLELLQRSQ
EVMRKYEIVANQVKYSVKDRWPETTGLLDYMKREGIALMAYTPLEKGTLARNE
CLAKIGEKYGKTAAQVALNYLIWEENVVAIPKASNKEHLKENFGAMGWRLSEE
DREMARRCVGSLVPRGSCRSNAVAEQGRKTQEFTQQSAQYVEAARKHYDAAE
KLNIPDYQEKEDAFMQLVPPAVGADIMRLFPEKSAALMYHLGANPEKARQLLA
MDGQSALIELTRLSERLTLKPRGKQISSAPPADQPITGDVSAANKDAIRKQMDAA
ASKGDVETYRKLKAKLKGIR

GFP-SP
MKGVKEVMKISLEMDCTVNGDKFKITGDGTGEPYEGTQTLHLTEKEGKPLTFSF
DVLTPAFQYGNRTFTKYPGNIPDFFKQTVSGGGYTWERKMTYEDGGISNVRSDIS
VKGDSFYYKIHFTGEFPPHGPVMQRKTVKWEPSTEVMYVDDKDGVLKGDVNM
ALLLKDGRHLRVDFNTSYIPKKKVENMPDYHFIDHRIEILGNPEDKPVKLYECAV
ARYSLLPEKNKELPWLVPRGSCRSNAVAEQGRKTQEFTQQSAQYVEAARKHYD
AAEKLNIPDYQEKEDAFMQLVPPAVGADIMRLFPEKSAALMYHLGANPEKARQ
LLAMDGQSARIELTRLSERLTLKPRGKQISSAPHAQPITGDVSAANKDAIRKQMD
AAASKGDVETYRKLKAKLKGIRLVGHHHHHH

SP-141
RSNAVAEQGRKTQEFTQQSAQYVEAARKHYDAAEKLNIPDYQEKEDAFMQLVP
PAVGADIMRLFPEKSAALMYHLGANPEKARQLLAMDGQSALIELTRLSERLTLK
PRGKQISSAPPADQPITGDVSAANKDAIRKQMDAAASKGDVETYRKLKAKLKGI
R

CelB-SP
MAKFPKNFMFGYSWSGFQFEMGLPGSEVESDWWVWVHDKENIASGLVSGDLP
ENGPAYWHLYKQDHDIAEKLGMDCIRGGIEWARIFPKPTFDVKVDVEKDEEGNII
SVDVPESTIKELEKIANMEALEHYRKIYSDWKERGKTFILNLYHWPLPLWIHDPIA
VRKLGPDRAPAGWLDEKTVVEFVKFAAFVAYHLDDLVDMWSTMNEPNVVYN
QGYINLRSGFPPGYLSFEAAEKAKFNLIQAHIGAYDAIKEYSEKSVGVIYAFAWH
DPLAEEYKDEVEEIRKKDYEFVTILHSKGKLDWIGVNYYSRLVYGAKDGHLVPL
PGYGFMSERGGFAKSGRPASDFGWEMYPEGLENLLKYLNNAYELPMIITENGM
ADAADRYRPHYLVSHLKAVYNAMKEGADVRGYLHWSLTDNYEWAQGFRMRF
GLVYVDFETKKRYLRPSALVFREIATQKEIPEELAHLADLKFVTRKQGSLVPRGS
CRSNAVAEQGRKTQEFTQQSAQYVEAARKHYDAAEKLNIPDYQEKEDAFMQLV
PPAVGADIMRLFPEKSAALMYHLGANPEKARQLLAMDGQSALIELTRLSERLTL
KPRGKQISSAPPADQPITGDVSAANKDAIRKQMDAAASKGDVETYRKLKAKLKG
IR

1. Kelley, L. A.; Mezulis, S.; Yates, C. M.; Wass, M. N.; Sternberg, M. J., The Phyre2 web portal for protein modeling, prediction and analysis. *Nature protocols* **2015,** *10* (6), 845.
2. Popot, J.-L.; Trewhella, J.; Engelman, D. M., Reformation of crystalline purple membrane from purified bacteriorhodopsin fragments. *The EMBO journal* **1986,** *5* (11), 3039-3044.